Cooperative Preassociation Stages of PEO−PPO−PEO Triblock Copolymers: NMR and Theoretical Study

Jaroslav Kříž* and Jiří Dybal

Institute of Macromolecular Chemistry AS CR, v. v. i., Heyrovského Sq. 2, 162 06 Prague, Czech Republic

Received: November 25, 2009; Revised Manuscript Received: February 2, 2010

Using ^{1}H and ^{13}C 1D and 2D NMR spectra, pulsed field-gradient (PFG) diffusion measurements, and ^{13}C relaxations supported by density functional theory (DFT) calculations, the temperature-dependent behavior of $(EO)_m(PO)_n(EO)_m$ block copolymers (m/n = 31/14, 31/72, and 17/1) in D_2O below and at the critical micellar temperature (CMT) was investigated in order to understand the nature of primary self-association acts and their true driving force. It was shown that a conformation change of the PO block followed by mild and reversible association with other PO blocks and eventually with the inner parts of EO blocks starts at temperatures 10−12 K below the CMT. The primary process is the entropy-driven disintegration of the PPO hydration envelope based on cooperation of hydrophobic hydration and hydrogen bonding. The partial dehydration of PPO is followed by its conformation change. Both processes are cooperative and reversible with a correlation time of the order 0.01 s and an activation energy of 51.3 kJ/mol. The PPO chain in a staggered conformation is prone to self-association starting at temperatures 5−6 K below CMT. In $(EO)_m(PO)_n(EO)_m$ block copolymers, this process is complicated by the stripping of PEO chains of a part of hydrogen-bound water and entwining them with PPO. It is shown that only inner (PPO-near) parts of PEO take part in the process, the end-groups remaining free.

Introduction

Ethylene oxide−propylene oxide (EO−PO) block copolymers commercially known as Pluronics or Poloxamers have been of scientific interest in the last two decades for their practical use as nonionic surfactants and potential carriers of less soluble substances but also, from the theoretical point of view, for their remarkable self-association and self-ordering behavior at higher temperatures and/or higher concentrations in water.[1–5] Special attention has been given to the symmetric triblock copolymers $(EO)_m(PO)_n(EO)_m$. Phase diagrams were obtained in a wide range of concentrations and temperatures, and prevailing morphology was attributed to individual phases using various scattering (DLS, SAXS, SANS) methods.[6–14] For symmetric copolymers $(EO)_m(PO)_n(EO)_m$ with $2m \geq n$ and concentrations <20% w/w, a shifting equilibrium between unimers and micelles with varying association numbers was generally found in the vicinity of the critical micellar temperature (CMT). Although some controversy still remains about the true structure (or rather morphology) of these micelles, there is a general agreement about their most apparent features: there certainly is a micellar core consisting mostly of PO blocks and a varying amount of trapped water; there is a corona in the outer part of the micelle made up of more hydrophilic PEO blocks and rendering the micellar associate its thermodynamic stability; and there is most probably an intermediate region of a varying thickness between the corona and the core, which consists of variously entwined EO and PO segments. This interesting phenomenon was better demonstrated in higher aggregates and liquid crystalline phases[6–8] using quadrupolar splitting in ^{2}H NMR of the trapped D_2O or ^{14}N spin electron splitting constants in a series of spin labels with increasing hydrophobicity.[14] The latter technique was able to demonstrate a less steep radial hydration gradient even in the coronas of individual micelles of symmetric $(EO)_m(PO)_n(EO)_m$ copolymers[14] with lower values of m ($2m \leq n$).

The various self-association phenomena in these copolymers motivated scrutiny of their thermally induced structural changes by spectroscopic methods, namely, vibrational spectroscopy[15–22,24] and NMR.[9,23] Changes in C−O−C stretching and CH_3 deformation frequencies were meticulously measured[24] over a broad temperature range in small intervals. The thermally induced decrease of the blue shift (compared to the neat copolymer) of the C−H deformation vibration indicates the loss of the organized hydrophobic-hydration envelope of the PO methyl groups, whereas the decrease of the red shift of the C−O stretching vibration shows the weakening or eventual loss of the hydrogen bonds with the surrounding water. The shape of these temperature dependences changes with the type of the copolymer. Abstracting from some interesting anomalies, one can say that the onset of the steepest part of the dependence and its inflection point (identified with CMT) shifts to higher temperature and its slope decreases with increasing m/n ratio; also, the heating−cooling hysteresis is usually less apparent, although there are other factors (such as the value of n) influencing it. When comparing the two curves for the same copolymer (e.g., PE6400 with m = 14 and n = 31), one can see that the steepest part for CH_3 vibration is in the range 30−50 °C, whereas that of C−O stretching starts around 30 but ends at about 68 °C. Evidently, EO units continue losing hydrogen bonds at temperatures at which PO units were already deprived of their water envelopes.

In addition to the loss of hydration caps (for CH_3 vibrations) or H-bonded water (for C−O−C vibrations), the thermally induced shifts could be partly caused by other effects, namely, conformation change[23,24] or (contrary to the opinion of the present authors) even the formation of an intramolecular CH−O hydrogen bond.

To some degree, the chemical shifts of CH_3 and CH_2 protons and carbons in ^{1}H and ^{13}C NMR spectra[23] appear to have similar trends as the wavelength of the just mentioned vibrations, although there are less data here for comparison. In general, the proton

10.1021/jp911205q
Published on Web 02/12/2010

signals are reported to move downfield and carbon signals conversely upfield when the copolymer adopts a micellar state. In addition to it, the chemical shifts appear to be strongly influenced in either state by the $2m/n$ ratio in the copolymer except for the region 0.8−1.2 where it seems to be almost constant. The main cause of the change of chemical shifts with temperature seems to be, according to the authors,[23] the thermally induced conformation change of the PPO segment. Some argument for it comes from a very thorough ^{13}C NMR and *ab initio* SCF study[25] of 1,2-dimethoxy-1-methylethane (DMME) as a low-molecular-weight model of PPO, although, when closely inspected, only one of the two C−O−C−H dihedral angles (inspected both by calculation and by $^3J_{CH}$ coupling constants), namely, CH_3-O-CH_2, exhibits some change in the temperature region 10−80 °C. However, taking the recommended[25] coefficients of the Karplus equation $a = 6.76$, $b = 2.71$, and $c = 2.07$ and the $^3J_{CH}$ values published in the graph, it is easy to find that the dihedral angle changes from 45.99° at 25 °C to a mere 43.63° at 75 °C in DMSO. Considering that the incident $^3J_{CH}$ coupling constant is somewhat uncertain (it is supposed to be the mean of the coupling constants of the two protons in the CH_2 group), the just mentioned change of the dihedral angle (a mere 2.3° over 50 °C) is not very impressive either. Does it mean that PPO does not exhibit considerable conformation change under heating, in particular in aqueous medium? We believe that a more natural answer is that the question remains open because DMME is a too simple model of PPO and the study was not (probably could not be) carried out in water.

Considering the above sketch of findings which have been published until now, we have to admit that we still have only a meager knowledge especially about the early stages which precede or start the self-association of EO−PO block copolymers even in their most understandable types, namely, $(EO)_m(PO)_n(EO)_m$ with $2m \geq n$. The reason why it is worth trying to understand more lies in the fact that these copolymers are still comparably simple examples of amphiphilic macromolecules with lower critical temperature (LCT) of their aqueous solutions. There is some hope that the knowledge gained in their case could be applied to some more complex and interesting cases.

The individual phenomena one could imagine in the temperature region just below and at LCT are the following: (1) demolition of the hydrophobic-hydration caps on the PPO methyl groups (entropy effect); (2) loosening or breaking of water−ether oxygen hydrogen bonds both on PPO and PEO segments (both entropy and enthalpy effect); (3) change of the prevailing conformation (or rather set of conformations) of PPO segment to a more hydrophobic one; (4) stabilizing the new conformation by inter- or intramolecular interactions; (5) self-association mostly due to hydrophobic interactions of the PPO segments; (6) entwining of partially dehydrated PEO segments with PPO. It is highly probable that at least processes 2−5 are mutually cooperative so that it is difficult to set a clear logical priority to any of them.

In the present study, we center our attention on Pluronic PE6400, which is an $(EO)_m(PO)_n(EO)_m$ copolymer with a medium-sized PO block ($n = 31$) and long enough EO blocks ($m = 14$) to ensure a "normal" behavior, i.e., unimeric solubility in D_2O at room temperature and critical micellar temperature (CMT) at about 313 K. However, we compare its behavior with other products, in particular PPO as such.

Experimental Section

Materials and Samples. The Pluronics PE6400 and Syn PE F68 were obtained from BASF as free samples, which we gratefully acknowledge. The EO−PPO−EO copolymer L32 and the PO octamer were purchased from Sigma-Aldrich. All of these materials were dissolved to 10% w/w in 99.9% D_2O. In the case of the Pluronics, the solutions were heated to 310 K and filtered through a 20 μm filter. All solutions were degassed and sealed under argon.

NMR Spectra and Other Techniques. ^1H and ^{13}C NMR spectra and relaxations were measured with a 600 MHz Bruker 600 Avance III spectrometer taking typically 16 scans for ^1H and 800 scans for ^{13}C NMR. Part of the measurements, in particular PFG diffusion experiments and dynamic relaxation experiments, were done on a 300 MHz Bruker Avance DPX300 spectrometer, the former using an additional BGU II gradient unit and a special water-cooled *z*-gradient probe. Basic ^{13}C transverse relaxation experiments were done at 150.94 MHz using the Carr−Purcell−Meiboom−Gill (CPMG) sequence[31,32] with a 1 ms delay between the π pulses, taking 2 k points in 800 scans for each of the 32 experimental points. The dynamic ^{13}C transverse relaxation experiments were done at 75.45 MHz using a sequence blending the DEPT45 polarization transfer and the CPMG sequence, namely, with $d_1 = 3$ s, $d_2 = 3.45$ ms, and

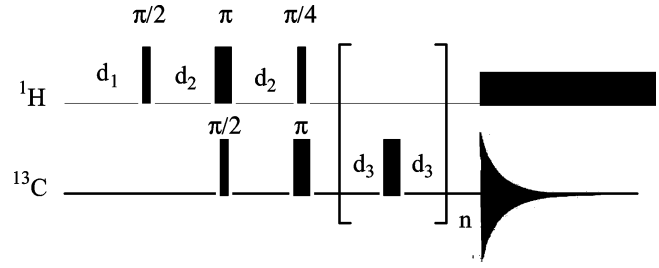

$d_3 = 2.0$, 1.5, 1.0, 0.5, 0.25, and 0.125 ms (for the spectrometer program of the sequence including phase cycling, see Supporting Information). 2056 points in 800 scans were taken for each of the 32 experimental points. The pulsed field-gradient (PFG) measurements of the diffusion coefficients were done using the improved[33] stimulated echo pulse sequence STE-LED2; the gradient pulse length was 1 ms, the diffusion delay Δ was 40 ms, and the gradient strength was increased in 16 steps up to 600 G/cm. 600 MHz ^1H NOESY spectra were measured with 400 ms mixing time taking 320 scans of 1028 points in 256 increments in an absolute mode. Before Fourier transform, both dimensions were transposed into 512×512 points and multiplied by a sine-bell weighting function.

Quantum Chemical Calculations. The model calculations were carried out at the density functional theory (DFT) level employing the Gaussian 03 program package.[34] All of the structures were fully optimized with the B3LYP functional and the 6-31G(d) and basis set.

Results and Discussion

1. NMR Spectra. Figure 1 shows ^1H and ^{13}C NMR spectra of 10% w/w solution of PE6400 in D_2O at 298 K. The signal assignment corresponds to Scheme 1 where the numbers of the protons are the same as those of the carbon atoms they are attached to. As seen from the spectra, the mostly atactic PPO block contains somewhat more *r* than *m* dyads. Unlike in vinyl polymers, the CH_2 protons are nonequivalent in the *r* dyad; their only apparent equivalence in the *m* dyad has not been explained in a quite satisfactory way.[23] Also, the *r* dyad can be considered to be somewhat more hydrophobic as the methyl groups point approximately in the same direction.

Figure 2A shows how the CH and CH_2 part of the ^1H NMR spectra changes with temperature well below CMT. Whereas no significant change can be seen in the CH_3 signal, there is a

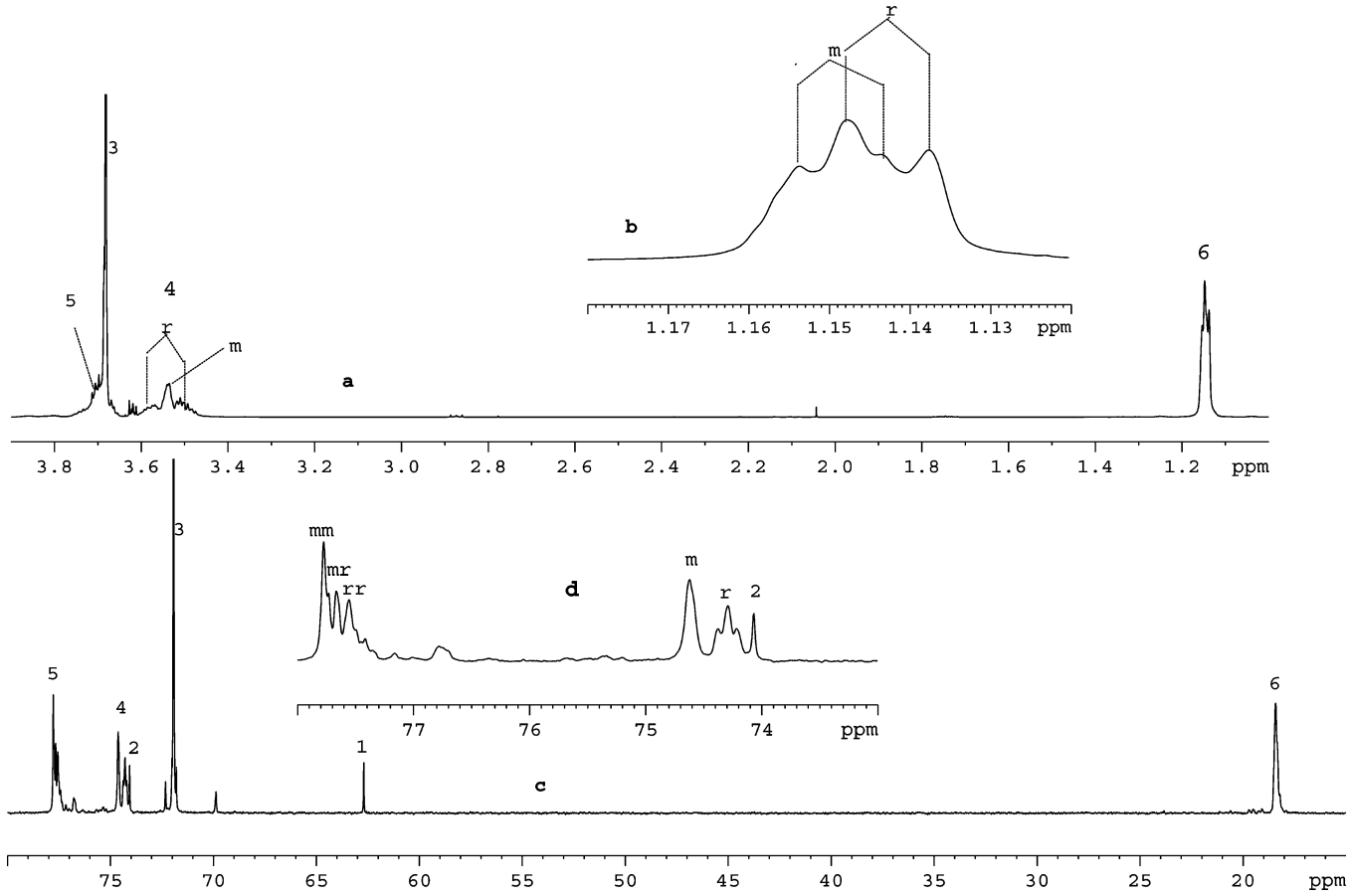

Figure 1. 600.2 MHz ^{1}H (a, b) and 150.94 MHz ^{13}C (c, d) spectra of a 10% w/w solution of PE6400 in D_2O at 298 K.

SCHEME 1

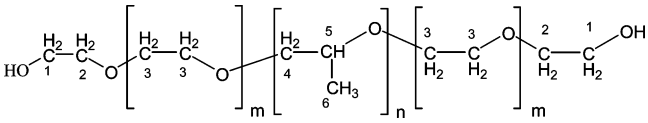

significant change in PO CH_2 signals (*r* dyad) already at 302 K, i.e., at least 10 K below the CMT.

A similar observation can be made in ^{13}C NMR spectra with the distinction that the changes are seen mostly in the CH_3 (or 6) signal. As seen in Figure 3a, the first signs of the change can be detected again at 302 K. The change of the signal is gradual, and comparing Figure 3a and b, one can see that the original signal 6 (marked as *a* in Figure 3b) (i) broadens and (ii) is gradually substituted by a 1.1 ppm downfield-shifted signal (marked as *b*) and, to a small degree, by a broad, 2.2 ppm downfield-shifted signal *c*.

From the fact that *a* and *b* are clearly distinct signals (their convolution being due only to their relative broadness), it is clear that the correlation time of exchange between the corresponding forms must be at least 20 ms. The dynamics of this exchange will be inspected below.

In ^{1}H NMR spectra, the main thermal change is that of signal 4 (PPO$-CH_2$) and signal 6 (PPO$-CH_3$) remains virtually unchanged in the given temperature region. In ^{13}C NMR, signal 6 is the most changing one, whereas the others (4, 5, and in particular 3) are much less affected. The primary cause of such behavior must be a major conformation change of the PPO block rather than, e.g., the change of its immediate environment which should affect all signals in approximately the same way. Now, as already indicated in the Introduction, two main possibilities offer themselves: (i) a purely thermal change of the conformation distribution leading to a more hydrophobic PPO shape or, conversely, (ii) a conformation change induced by the thermal change of the PPO−water interaction. Although the first possibility (i) is not probable considering the model calculations,[25] we decided to explore it on PPO itself.

Unfortunately, PPO of any longer chain length is very poorly soluble in water. However, inspecting PPO ($P_n = 35$) in $CDCl_3$ and dimethylsulfoxide-d_6, we did not find any significant change of its ^{1}H and ^{13}C NMR spectra (10% w/w solution) between 298 and 323 K (see the Supporting Information, Figure 1). Thus, the purely thermal behavior of PPO itself clearly cannot be the cause of the observed phenomena.

In order to check up the second possibility (ii), we used a PPO oligomer ($P_n = 8$) soluble in water. To some surprise, its spectra again did not show any detectable change up to 328 K (see the Supporting Information, Figure 2). Suspecting that the length of the PPO chain could have significance in the inspected behavior, we chose a copolymer of an approximate composition $(EO)_1(PO)_{17}(EO)_1$ (purchased as Pluronic L31), i.e., a product with a double length of the PPO chain and a lowest possible influence of EO chains. Owing to the range of its solubility, we started to measure this product at 291 K but had to go even over its clouding temperature (300 K) to compare it with PE6400 (see Figure 2B). As seen, signal 4 has an analogous tendency to shift upfield but is somewhat more reluctant to do so. Over 306 K, most of the copolymer forms a heterogeneous phase and is not seen in the spectrum. To sum up this part of the experiments, 17 apparently is just about the number of propylene oxide (PO) units at which the tendency of the PPO block to form a more staggered conformation starts.

When the length of the PPO block is sufficient (i.e., $n > 22$) but the length of the PEO block is markedly increased (from $m = 14$ in PE6400 to $m = 72$ in F68), the thermal change of the ^{13}C signal 6 is quite analogous but shifted about 6 K to higher temperatures (see the Supporting Information, Figure 3). Evidently, the "hydrophilic pull" of the longer PEO chain affects the tendency of the PPO block to dehydrate and adopt a more staggered conformation (see the discussion of this effect in the comprehensive discussion below).

2. Inspection of the Molecular Size by PFG Diffusion Measurements. If the PPO conformation change observed in the EO−PO−EO copolymers means coiling of PPO in the preassociation state, this phenomenon should be reflected (however slightly) in the effective size of the molecule. Assuming that we are allowed to use the Stokes−Einstein relation for the translation diffusion coefficient

$$D = \frac{kT}{6\pi R_H \eta} \tag{1}$$

where k is the Boltzmann constant, T the absolute temperature, and η the viscosity of the medium, we can obtain the effective hydrodynamic radius R_H from the self-diffusion coefficient measured by PFG NMR. There are two main problems of this approach. First, the self-diffusion coefficient is obtained by measuring the dependence of integral NMR signal intensity I on the field gradient g applied in a pulse of length δ, using the formula

$$I = I_0 \sum_{i=1}^{n} w_i \exp\left[-\gamma^2 g^2 \delta^2 (\Delta - \delta/3) D_i\right] \tag{2}$$

where γ is the gyromagnetic ratio of the given nucleus (proton in our case), Δ is the diffusion delay in the pulse sequence, and D_i and w_i are the self-diffusion coefficient of the ith species and its statistical weight, respectively. If the species is uniform in size or there is fast exchange between analogous species with different size, $n = 1$, $w_1 = 1$, and D_1 is simply the self-diffusion coefficient of the species. However, given a wider size distribution of species and slow or missing exchange between them, we obtain a multiexponential decay (i.e., $n > 1$ in eq 1). Contrary to some implicit claims present in the literature, it is rather difficult to obtain exact and meaningful values of the coefficients w_i if the decay is polyexponential and in particular if there is slow exchange between the individual species. In our experiments, we obtained either monoexponential decays for $(PO)_8$ (all temperatures) and PE6400 (298 K). In other cases, the decays were apparently biexponential. As both w_i and D_i values are probably affected by exchange between the species, we used either the prevailing component or the "effective coefficient" D_{ef} defined as

$$D_{ef} = \sum_{i=1}^{n} w_i D_i \tag{3}$$

for the calculation of R_H. D_{ef} has no strict physical meaning and serves mainly for illustrative purposes. Table 1 collects the

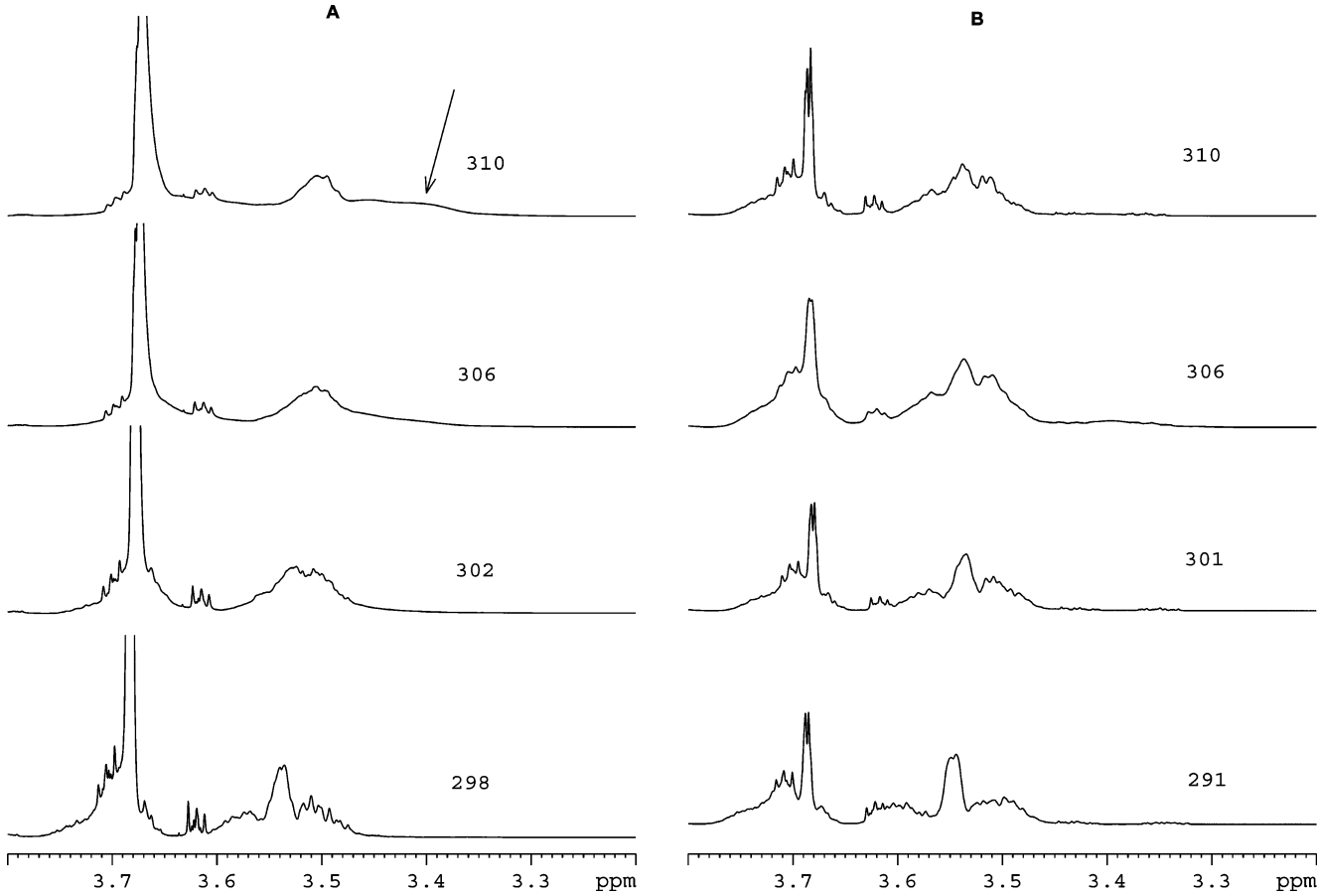

Figure 2. CH and CH_2 region of the ^1H NMR spectra of 10% PE6400 (A) and L31 (B) in D_2O at the indicated temperatures.

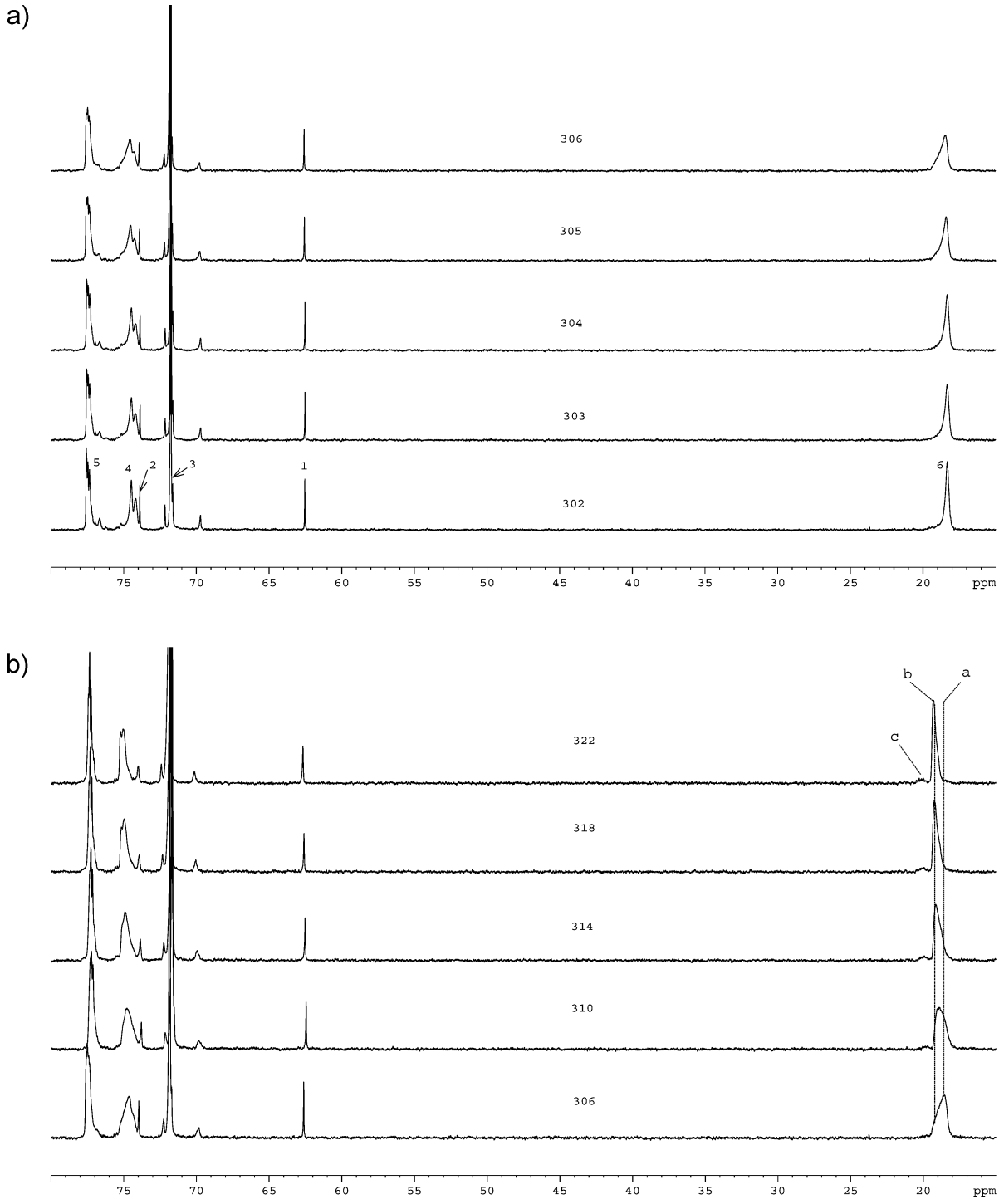

Figure 3. (a) 150.94 MHz ^{13}C NMR spectra of 10% D_2O solution of PE6400 at the indicated temperatures. (b) 150.94 MHz ^{13}C NMR spectra of 10% D_2O solution of PE6400 at the indicated higher temperatures.

values of D_i obtained by mono- or biexponential fitting and the calculated values of D_{ef}.

The second problem with the diffusion measurements is the temperature dependence of D due to the linear (kT) and exponential (η) terms in eq 1. As both terms are the same for the measured sample and the water medium (the residual HOD signal), we take as a molecular-size-related quantity, comparable over the whole temperature region, a water-relative hydrodynamic radius $R_{H\mathrm{rel}}$ defined as

$$R_{H\mathrm{rel}} = R_{Hj}/R_{Hw} = D_w/D_j \qquad (4)$$

where the index j can mean either i in the polyexponential fit or ef according to eq 3. As neither the water molecule nor the copolymer are spherical objects, $R_{H\mathrm{rel}}$ is not a relative radius in a strict sense; however, with both objects being the same in the given temperature region, it can serve as a semiquantitative measure of the copolymer size. The values for PE6400 and oligomeric PPO are plotted in Figure 4.

As one can see, the PO oligomer does not change its size in the whole temperature range, which is in full agreement with the absence of any change in its NMR spectra. For PE6400, there are two components of D starting with 306 K. In both,

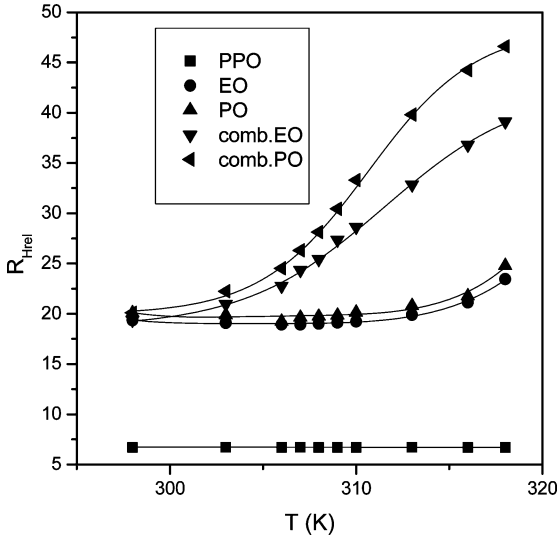

Figure 4. Temperature dependence of hydrodynamic radii (relative to water) of PPO octamer and PE6400, namely, from the prevailing component of D measured on signals 3 (EO) and 6 (PO) and values obtained from D_{ef} for signals 3 (EO comb.) and 6 (PO comb.), respectively.

we observe a difference between the measurements using signal 3 (EO) or 6 (PO), which is given most probably by a slight chemical inhomogeneity of the copolymer (the molecules with higher PPO content diffusing slower and associating earlier). The faster components of D converted to R_{Hrel} are plotted as EO and PO in Figure 4. As we see, the R_{Hrel} value very slightly decreases between 298 and 310 K. Taking into account the exchange between the unimer and preassociated forms (see below) which somewhat shifts the D values of the fast and slow component nearer to each other, we can assume that the real decrease of R_{Hrel} should be somewhat larger; i.e., we observe the conformation change of the PPO part of the copolymer.

The combined values of R_{Hrel} derived from D_{ef} and shown in Figure 4 clearly show that preassociation already starts at 303 K. The increase of R_{Hrel} of the unimeric components above 313 K combined with the decreasing slope of the combined curves is one of the signs of exchange between the unimers and the early associates. We are going to inspect the dynamics of this exchange in a separate paragraph.

3. Investigation of the Interactions Using the Nuclear Overhauser Effect (NOE). Another way to inspect conformation change of the PPO part of the copolymer is the utilization of NOE. Unfortunately, as Figure 5 shows, the broadening of signals 4 and 5 at temperatures over 306 K leads to corresponding widening of the cross-peak with signal 6 precluding thus an unequivocal comparison. Nonetheless, NOESY spectra proved valuable in another way. Somewhat unexpectedly, cross-peaks between the residual signal of water (HOD) and signals 3 and 6 can be observed at both 298 and 310 K, documenting spatial nearness of water to both CH_2OCH_2 groups of PEO (due to H-bonds to the oxygen atom) and CH_3 groups of PPO (due to hydrophobic hydration). The remarkable thing is that the residence of a water molecule within 0.4 nm from the given proton of the copolymer must not be shorter than about 10^{-6} s to get such an effect we observe.[26] Thus, relatively stable hydration structures must exist even at 310 K. However, the ratio of integral intensities of the HOD cross-peaks with 3 and with 6 is 1.62 at 298 K but 2.73 at 310 K. Evidently, the hydrophobic hydration of the PO methyl groups decays at lower temperatures than the hydrogen bonds with EO oxygen atoms do. This is in excellent accord with the thermal development of infrared spectra.[24] The fact that we come to the same conclusion on grounds of a physically quite different phenomenon gives it additional weight.

TABLE 1: Diffusion Coefficients (10^{11} m^2 s^{-1}) and Their Weighting Coefficients Measured at Signals 3 (EO) and 6 (PO) of PE6400 in D_2O

	EO					PO				
T (K)	w_1	D_1	w_2	D_2	D_{ef}	w_1	D_1	w_2	D_2	D_{ef}
298	1.00	9.27			9.27	1.00	8.93			8.93
303	0.89	10.16	0.11	2.16	9.28	0.87	9.77	0.13	1.82	8.74
306	0.80	10.85	0.20	1.80	9.04	0.76	10.69	0.24	1.11	8.39
307	0.74	11.18	0.26	1.68	8.71	0.72	10.79	0.28	1.04	8.06
308	0.72	11.47	0.28	1.15	8.58	0.68	11.05	0.32	0.77	7.76
309	0.68	11.47	0.32	0.69	8.02	0.64	11.06	0.36	0.67	7.21
310	0.66	11.48	0.34	0.39	7.71	0.59	10.92	0.41	0.60	6.63
313	0.60	12.09	0.40	0.19	7.33	0.50	11.57	0.50	0.53	6.06
316	0.57	11.94	0.43	0.13	6.86	0.47	11.62	0.53	0.47	5.71
318	0.59	11.23	0.41	0.25	6.73	0.51	10.63	0.49	0.46	5.65

4. Investigation of the Local Mobility of PPO Block by Transverse ^{13}C NMR Relaxation. It is known[27] that, although even longitudinal relaxation reflects motional dynamics of polymer molecules, transverse relaxation is much more sensitive to slight changes of the local mobility of groups. We chose the ^{13}C NMR relaxation because ^{1}H NMR does not give sufficient resolution of all signals even at 600 MHz. In this paragraph, we used the single-pulse excitation before the CPMG train to be sure that no additional effects could complicate the results.

Let us take the PPO part of the spectrum first. Whereas the longitudinal relaxation is apparently monoexponential, transverse relaxation shows biexponential decays starting with 304 K. The results corresponding for transverse relaxation to the general relation

$$I = I_0 \sum_i w_i \exp(-t/T_{2i}) \qquad (5)$$

are given in Table 2 and partly illustrated in Figure 6.

The decays in the inversion−recovery experiments (T_1) were monoexponential, whereas the decays in the experiments with CPMG sequence (T_2) were apparently biexponential above 302 K (see examples in Supporting Information, Figures 4 and 5).

In a semiquantitative agreement with diffusion experiments (paragraph 2), the much faster relaxing component in transverse relaxation, the weight of which increases with temperature, probably corresponds to premicellar aggregates. Our chief concern, however, is the main component reflecting the behavior of the nonassociated PPO block.

As seen in Figure 6, only signal 5 exhibits a marked increase in transverse relaxation rate (decrease of T_2) with increasing temperature; that of signal 4 remains almost unchanged and that of signal 6 shows even a substantial decrease, indicating thus higher mobility. This, however, is not a true picture of the local mobility. We encounter here the same problem as we had with diffusion: with increasing temperature, the viscosity of the system decreases and the motion of the whole copolymer molecule is more thermally agitated. To get a purified picture, we propose the following analysis.

Let us assume for the sake of simplicity that the relaxation mechanism is purely dipolar and no motional hindering takes place. Then, both ^{13}C longitudinal and transverse relaxation are exponential and their rates R_1^C and R_2^C are described[28] by the

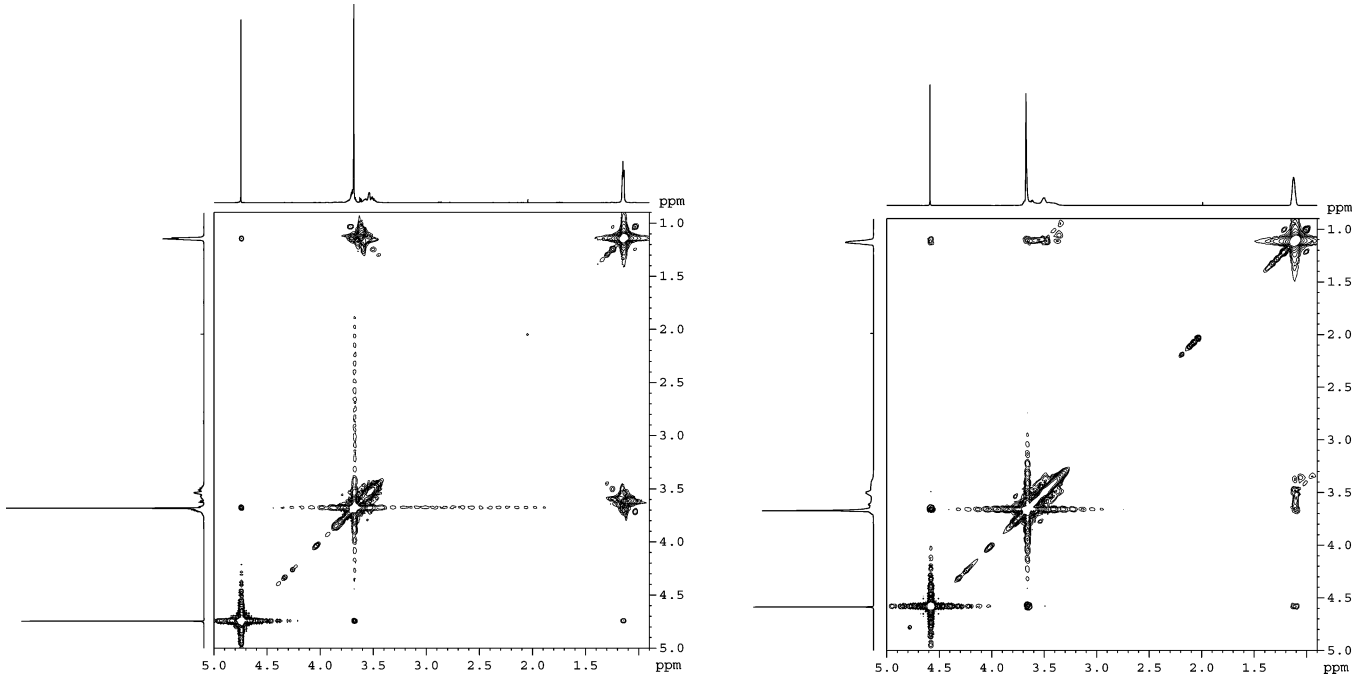

Figure 5. ^{1}H NOESY spectra of the 10% solution of PE6400 in D_2O at 298 K (left) and 310 K (right).

TABLE 2: Values of T_1 and T_{21} and T_{22} Components of T_2 (All in s) with the Weights w_1 of T_{21} ($w_2 = 1 - w_1$) for Signals 4, 5, and 6 in PE6400

	signal 4				signal 5				signal 6			
T (K)	T_1	w_1	T_{21}	T_{22}	T_1	w_1	T_{21}	T_{22}	T_1	w_1	T_{21}	T_{22}
298	0.482	1.00	0.287		0.369	1.00	0.210		0.655	1.00	0.397	
302	0.491	1.00	0.279		0.376	1.00	0.205		0.715	1.00	0.431	
304	0.497	0.92	0.279	0.032	0.379	0.91	0.205	0.020	0.751	0.95	0.444	0.076
306	0.507	0.89	0.276	0.028	0.382	0.87	0.203	0.016	0.787	0.88	0.455	0.067
308	0.515	0.87	0.275	0.028	0.384	0.85	0.200	0.014	0.819	0.87	0.463	0.052
310	0.522	0.84	0.273	0.026	0.389	0.83	0.201	0.012	0.853	0.84	0.469	0.045
312	0.527	0.80	0.270	0.023	0.394	0.79	0.194	0.010	0.880	0.81	0.468	0.034
314	0.537	0.78	0.268	0.018	0.396	0.73	0.188	0.008	0.915	0.79	0.469	0.028
318	0.562	0.69	0.267	0.015	0.406	0.65	0.185	0.006	0.977	0.72	0.479	0.020
322	0.596	0.61	0.273	0.010	0.426	0.56	0.187	0.002	1.044	0.68	0.497	0.017

equations (ω_C and ω_H being the Larmor frequencies of ^{13}C and ^{1}H, respectively)

$$R_1^C = \mathbb{R}[6(\omega_C + \omega_H) + 3J(\omega_C) + J(\omega_H - \omega_C)] \quad (6)$$

$$R_2^C = \mathbb{R}[3J(\omega_C + \omega_H) + 3J(\omega_C)/2 + 3J(\omega_H) + J(\omega_H - \omega_C)/2 + 2J(0)] \quad (7)$$

with

$$\mathbb{R} = (1/20)(\mu_0/4\pi)^2(\gamma_C\gamma_H\hbar/r_{CH}{}^3)^2 \quad (8)$$

where μ_0 is the vacuum permittivity, γ_C and γ_H are the ^{13}C and ^{1}H gyromagnetic ratios, respectively, and r_{CH} is the distance between the ^{13}C and ^{1}H nuclei. The spectral density functions $J(\omega_X)$ in the case of unhindered random rotational diffusion are

$$J(\omega_X) = \frac{\tau_c}{1 + (\tau_c\omega_X)^2} \quad (9)$$

where τ_c is the correlation time of the main motion causing relaxation.

Let us assume that τ_c is about 1.0×10^{-9} s at 298 K (a probable value considering the measured T_1) and its decrease with increasing temperature is exponential.

$$\tau_c = \tau_0 \exp(\Delta E/RT) \quad (10)$$

A reasonable value of the activation energy ΔE should be 33.5 kJ/mol (8 kcal/mol). Using eqs 6, 7, 8, and 9, we can calculate the ratio $\rho = R_2/R_1$ for the temperatures of our measurements. As shown in Figure 7, the theoretical value of ρ under assumed constants (denoted t in the figure) decreases, converging to 1 at very high temperatures; at reasonably higher ΔE, the dependence ρ on T would be slightly different but analogous. However, as we see in Figure 7, the experimental dependences are quite different, showing quite a marked increase of ρ with increasing temperature. This is evidence that the PPO block undergoes a *relative* decrease of its local mobility with increasing temperature probably caused by its conformation change.

5. Investigation of the Dynamics of the Conformational Change. From the shape of the ^{13}C NMR signal 6 in Figure 2, it is clear that the exchange between the original and the preassociated form of the PPO block cannot be fast. However, to be sure that there is exchange at all, as we assumed above,

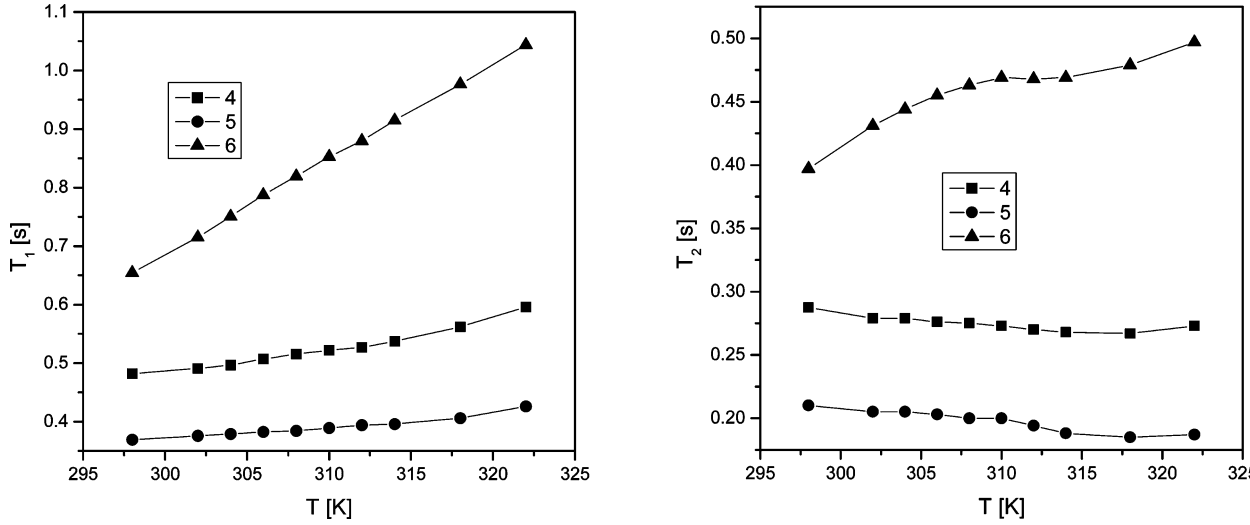

Figure 6. Values of T_1 (left) and T_2 (main component, right) measured for the indicated ^{13}C NMR signals at 150.94 MHz and the given temperatures.

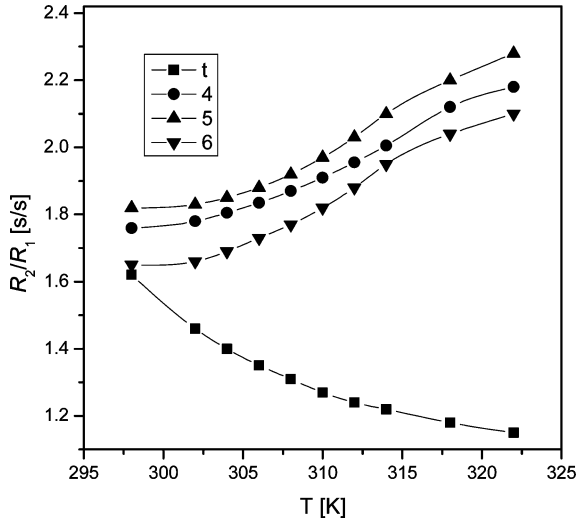

Figure 7. Theoretical (t) and experimental values of R_2/R_1 for the indicated ^{13}C NMR signals of PE6400 at 150.94 MHz and the given temperatures.

one has to demonstrate it by measuring its rate. This is not easy for various reasons: the signals of the two forms are too near to each other for applying the selective-saturation method; on the other hand, the method using the variation of the interpulse delay in CPMG sequence needs a homogeneous signal for unequivocal results. For the latter reason, we made the following measurement with a 300 MHz NMR instrument, i.e., at 75.45 MHz, where the components of the signal are less resolved. To make up for the lower sensitivity, we used a blend of DEPT45 and CPMG sequence (its program for Bruker spectrometers is in the Supporting Information). The side-effect of this arrangement was that the decays were apparently monoexponential. This facilitated the analysis on the expense of the fast-relaxing component observed at higher temperatures (see above), which probably was filtered off (this signal-narrowing effect of polarization-transfer techniques was observed by us many times in the past and is caused both by the less efficient polarization of broad proton signals and by relaxation during the delays of the DEPT or INEPT sequence).

Irrespective to the means of ^{13}C polarization, its transverse relaxation rate under chemical exchange with the correlation time τ_{ex} should obey the relation[29]

$$R_2(t_p) = R_2^0 + p_1 p_2 \delta\omega^2 \tau_{ex}[1 - (\tau_{ex}/t_p)\tanh(t_p/\tau_{ex})] \quad (11)$$

where p_1 and p_2 are the probabilities of the exchanging sites, $\delta\omega$ is the relative chemical shift in rad/s, and t_p is the delay between the π pulses in the CPMG part of the sequence. As the expected τ_{ex} is comparable to t_p, no approximation[30] to eq 11 can be used.

The value of $\delta\omega$ is 379.3 rad/s at 75.45 MHz. The values of p_1 and p_2, obtained by signal deconvolution at 150.94 MHz, are given in Table 3 together with the values of τ_{ex} and R_2^0 fitted to the experimental values of R_2 shown in Figure 8.

The values of τ_{ex} obtained in this procedure are reasonable, although somewhat larger values were expected (it is possible that the filtering off of the fast-relaxing components produces some systematical bias). As shown in Figure 9, the obtained values of τ_{ex} give a reasonable Arrhenius plot with the slope 6.134×10^3, the activation energy of exchange 51.3 kJ/mol. This rather low value shows that the barrier of exchange between the original and staggered forms of the PPO block (which is in a feedback relation with its dehydration) is rather that of entropy than of energy.

6. Investigation of the Local Mobility of PEO Blocks by Transverse ^{13}C NMR Relaxation. As already said in the Introduction, PE6400 is one of the PEO−PPO−PEO copolymers in which the PEO corona undergoes an interesting change[14] due to gradual loss of hydrogen bonds with water with increasing temperature. The crucial question is whether the prevailing mode of change is a gluing of whole PEO blocks into bundles or the inner parts of PEO get entwined with PPO core, leaving their outer parts virtually free. The use of variously hydrophilic spin probes in ESR could not clearly decide the

TABLE 3: Values of p_1 and p_2 and the Exchange Correlation Time τ_{ex} (in ms) and R_{20} Fitted to the Experimental Dependences of R_2 of Signal 6 of PE6400 on t_p at the Given Temperatures T

T	p_1	p_2	τ_{ex}	R_{20}
304	0.18	0.82	8.1	1.33
306	0.38	0.62	7.1	1.27
308	0.51	0.49	6.3	1.22
310	0.64	0.36	5.5	1.17
314	0.79	0.21	4.3	1.09

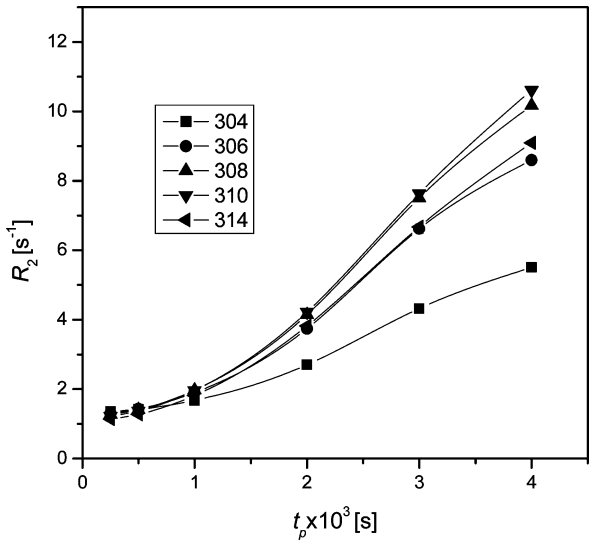

Figure 8. Dependence of the transverse relaxation rate R_2 of signal 6 in PE6400 on the delay t_p in CPMG sequence at the indicated temperatures (relaxation measured at 75.45 MHz).

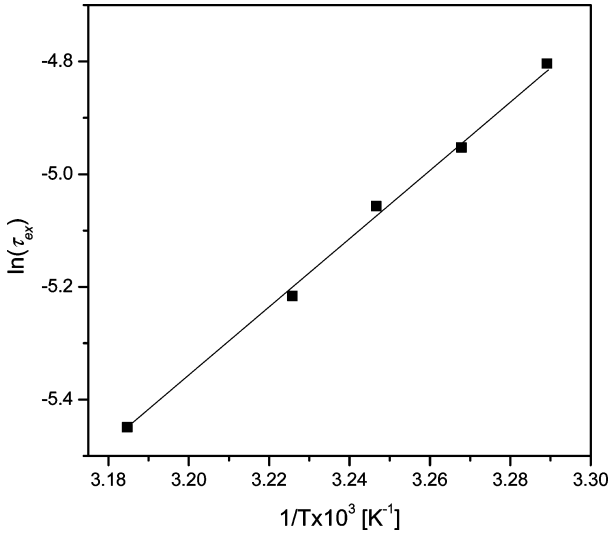

Figure 9. Arrhenius plot of the measured exchanged correlation time τ_{ex} of signal 6 in the ^{13}C NMR spectrum of PE6400.

problem, although the results rather pointed to the latter possibility.[14] ^{13}C NMR has the advantage that the terminal carbon of the PEO block has a separate signal 1 so that this question can be solved using ^{13}C NMR transverse relaxation, i.e., the same method as in paragraph 4. Table 4 shows the obtained results, which are also illustrated in Figure 10.

TABLE 4: Experimental Results of T_2 or Components T_{2i} (All in s) and Their Weights w_i in the Polyexponential Decay of ^{13}C Signals 1 and 3

	signal 1	signal 3					
T (K)	T_2	w_1	T_{21}	w_2	T_{22}	w_3	T_{23}
298	0.554	1.00	0.321				
302	0.643	1.00	0.373				
304	0.715	1.00	0.415				
306	0.795	0.87	0.461	0.13	0.138		
308	0.894	0.81	0.518	0.19	0.155		
310	0.996	0.76	0.578	0.24	0.173		
312	1.102	0.64	0.639	0.28	0.192	0.08	0.057
314	1.207	0.59	0.700	0.31	0.210	0.10	0.063
318	1.447	0.53	0.839	0.32	0.252	0.15	0.076
322	1.745	0.45	1.012	0.33	0.304	0.22	0.091

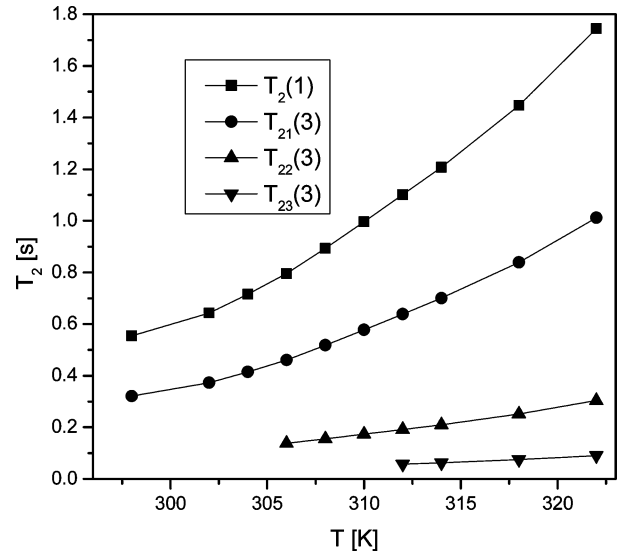

Figure 10. T_2 and T_{2i} values for signals 1 and 3 in the 150.94 MHz ^{13}C NMR spectrum of PE 6400.

As shown, the relaxation of the main PEO signal 3 gradually becomes polyexponential, whereas that of signal 1 (end-group of PEO) remains intact. The T_2 thermal development of signal 1 suggests almost free motion and nearly the same could be said about the slow-relaxing component T_{21} of signal 3.

Generally speaking, the polyexponentiality of transverse relaxation decay could be caused by the presence of a plurality of species with the same chemical shift but different mobility but also by the restricted motion[27] of one end of a chain (in which case the sum of exponentials is in fact an approximation to the nonexponential decay). The fact that the relaxation of signal 1 remains monoexponential shows that the outer end of PEO is relatively far from the hindered parts, which amounts to the evidence that PEO blocks gradually get entwined with PPO starting with their inner parts, leaving the outer parts free up to relatively high temperatures.

The interesting fact is that motional hindering of PEO clearly starts around 306 K, i.e., 7 K below the CMT. This shows that reversible preassociation takes place before proper polymer micelles are formed.

7. Theoretical Calculations of the Interaction of Water with PPO. In order to increase the precision of our experimentally based conception of interactions between W and the PPO chain, we turned to theoretical calculations. In principle, there are two possible approaches to such simulations: either to immerse mentally a PPO chain into a bath of hundreds of W molecules and simulate the interactions using approximate calculation methods such as molecular dynamics or take a small section of the chain and examine its interactions with a smaller number (such as 31 in our case) of W molecules as the first hydration shell, using a reliably precise method such as *ab initio* DFT calculation. Both approaches have their merits, but a long experience with comparing our spectroscopic data with theoretical predictions made us prefer the second approach. We have to acknowledge that the presence of further W molecules surrounding our model system as well as the general polarity of the medium could bring about some corrections to our simulated structure optimized *in vacuo*. However, many examples[35–39] of our previous calculations which gave satisfying predictions of experimentally observed vibration frequencies or NMR chemical shifts give us assurance that such corrections would not change the general features of the structure obtained

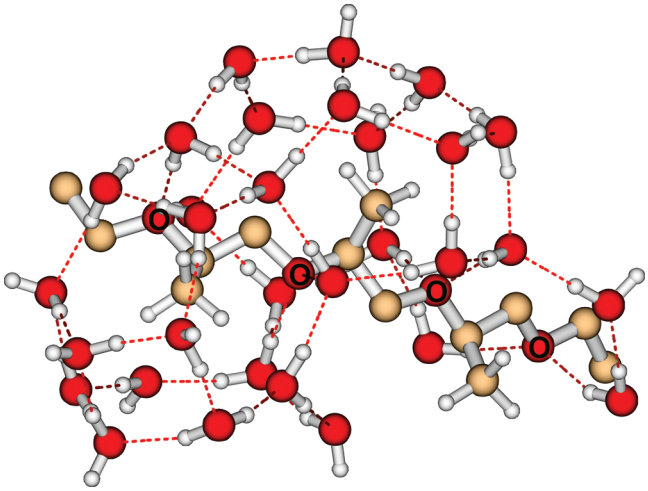

Figure 11. PPO segment interacting with surrounding water molecules: strong hydrogen bonds of water molecules with ether oxygen atoms (O) and hydrophobic cage-like structures around two of the methyl groups. Hydrogen atoms of PPO except of methyl groups are omitted for clarity.

by our method. We also would be glad to use a much longer PPO oligomer, but with all of the water molecules around it, the trimer was the largest system our three-processor computer was able to deal with; one energy optimization took 14 days and the whole computation about 2 months.

In our calculations, no *a priori* hypothesis of the form of the PPO trimer (with CH_3CH_2O endings approximately simulating the continuation of the chain) and the configuration of the 31 W molecules was made. Its geometry was fully energy-optimized without any geometrical constraints. The geometry corresponding to the lowest energy is shown in Figure 11. Two other local minima with somewhat higher energies were found, which repeated the general geometrical features of the global minimum, but the mutual orientations of W molecules were somewhat different. After a slight perturbation of their structure, their geometry converges to that shown in Figure 11.

The figure shows a strongly cooperative system of W molecules surrounding the methyl groups in a tight cage (the geometry of which amounts to a weak interaction, in agreement with infrared data) and wrapping up the neighboring ether groups as well. There are hydrogen bond interactions with these groups but only as a part of the whole cooperative hydrating system.

This hydration system is stabilized by bonding energy, mainly because of the hydrogen bonds between W molecules, which are statistically more numerous than in bulk water. From the thermodynamic point of view, it relies on enthalpy but is strongly negative-entropy demanding. The increase of this demand is disproportional to the length of the hydrated chain; hence, the disruption of the hydrating envelope by increasing temperature is much easier for longer PPO chains.

8. Comprehensive Discussion of the Results. As the techniques used here are numerous and we partly rely on results published elsewhere,[24] we feel the need for the following summarizing discussion. It has to start with the thermodynamics of the PPO block being immersed in water. Assume we put a monomeric unit PO into surrounding water (W). It makes a "hole" in it; i.e., it perturbs its natural structure which is, however, dynamic, stabilized by hydrogen bonds (HB) between individual W molecules. If we ignore for the moment the positive dipolar or van der Waals interactions between PO and W, which make only small corrections, the dissolution of a PO unit in W thus has some enthalpic requirement ($\Delta H_{sol} > 0$). At the same time, the dissolution of PO brings about entropic gain by randomizing its positions ($\Delta S_{sol} > 0$). Let us define ΔH_{sol}^{P}, ΔS_{sol}^{P}, and all other thermodynamic quantities discussed further as specific for one PO unit (we use the superscript P to distinguish it from an analogous increment for $(EO)_n$ discussed further on). Now, if we gradually connect an increased number of PO units into a $(PO)_n$ chain (keeping the PO concentration constant), the perturbation of water structure disproportionately increases (so that $(\Delta H_{sol}^{P})_n/n$ increases), whereas the entropy gain $(\Delta S_{sol}^{P})_n/n$ decreases. Consequently, there will be some limiting n for $(PO)_n$ at which the PO oligomer will be soluble at a given temperature.

There are some corrections to this coarse picture, however. First, we know from infrared spectra[24] that W molecules bind to ether oxygen atoms of $(PO)_n$ by hydrogen bonds somewhat stronger than to other W molecules, i.e., $\Delta H_{hb}^{P} < 0$. At the same time, the mobility of W molecules is relatively decreased by these bonds so that $\Delta S_{hb}^{P} < 0$. We also know from infrared spectra[24] and present calculations that W molecules tend to form a tightly organized cap around the PO methyl groups. This hydrophobic hydration is *locally* energetically advantageous (i.e., $(\Delta H_{hh}^{P})_n/n < 0$) but, of course, disadvantageous from the point of view of entropy ($(\Delta S_{hh}^{P})_n/n < 0$).

Thus, we can provisionally define the total change of the Gibbs energy of the dissolution of a $(PO)_n$ block as

$$\begin{aligned}(\Delta G)_n &= (\Delta G_{sol}^{P})_n + \sum_n [(\Delta G_{hb}^{P})_i + (\Delta G_{hh}^{P})_i] \\ &= (\Delta H_{sol}^{P} - T\Delta S_{sol}^{P})_n + \sum_n [(\Delta H_{hb}^{P} - \\ &\quad T\Delta S_{hb}^{P})_i + (\Delta H_{hh}^{P} - T\Delta S_{hh}^{P})_i] \end{aligned} \quad (12)$$

In order to make $(\Delta G)_n$ comparable for various n, it should be normalized by dividing it by n; as the same applies to the other side of the equation, we drop it. The sums of the contributions from the individual PO chain units on the right side of eq 12 could be substituted by multiplying by n if the corresponding thermodynamic contributions were additive. However, it probably is not the case. Model calculations in the preceding paragraph show (as they did when inspecting simpler amphiphilic systems[35]) that the water molecules in the hydrophobic-hydrating caps of the methyl groups and those bound by hydrogen bond to the nearby ether groups from a cooperative system extending along the whole PPO chain if both its length and temperature are low enough. This makes hydration thermodynamically advantageous if n is small but, due to entropy requirements, less so with increasing n.

As usual, keeping ΔG negative (as needed for a stable system) at increasing temperature is a trade-off mostly between enthalpic and entropic terms. $(\Delta G_{sol}^{P})_n$ generally increases with increasing n but decreases with increasing temperature. ΔG_{hb}^{P} and ΔG_{hh}^{P} are both negative at low temperatures but increase to zero under heating due to their negative entropic terms (formally possible positive values at even larger temperatures do not occur, as both hydrophobic hydration and hydrogen bonding vanish under such conditions). According to infrared data,[24] an increase of $(\Delta G_{hh}^{P} + \Delta G_{hb}^{P})_n$ is detectable at 302 K (or even lower for a bare PPO chain of sufficient length). The change is quite dramatic in the region 305−318 K. Our NMR results confirm this finding: $(\Delta G_{sol}^{P})_n$ apparently is sufficiently low for $n = 8$ to maintain the molecule virtually unchanged up to 328 K. Starting approximately with $n = 17$ (product L31), the loss of negative

$(\Delta G_{hh}^{P} + \Delta G_{hb}^{P})_n$ at temperatures above 305 K leads to gradual change of the state of the chain, primarily its adopting a more staggered conformation and secondarily associating with several other chains, both processes evidently decreasing the area of contact of PPO with W and thus lowering the value of ΔH_{sol}^{P}.

Infrared data show[24] that for $(PO)_{22}$ the disintegration of methyl-hydration caps and stripping of the ether bonds of the hydrogen-bound water is equally swift at temperatures between 292 and 294 K. This leads to two important conclusions: (i) the slower loss of W−ether H-bonds in PEO−PPO−PEO copolymers with temperature is due to their larger persistence in the case of PEO (neither IR nor NMR can distinguish them from those to PPO); (ii) the observation assures us (as our calculations do) that a system of cooperative interactions (HH and HB) exists along the whole PPO (either block or bare chain) as far as entropy allows it, i.e., at low temperatures. The entropy requirements of such a system depend strongly on the length of the chain, which is one of the reasons why $(PO)_8$ remains intact up to 320 K, $(PO)_{17}$ changes start at 302 K, and $(PO)_{22}$ dehydrates around 293 K.

Interestingly, the change to a staggered, slightly coiled conformation is a reversible process (similarly as the primary dehydration of the PO groups must be); i.e., there is a relatively slow but measurable exchange between the original and the staggered forms of $(PO)_n$, as we demonstrated by our dynamic examination of the product PE6400. Whereas the equilibrium between the former and the latter forms markedly shifts to the right between 302 and 314 K, the rate of exchange between them does not increase very much with increasing temperature. The activation energy of the process is about 50 kJ/mol, as one could expect for a conformation change with some hindrance. The rate thus must be mostly governed by activation entropy.

Before concluding this part concerning $(PO)_n$ as such, we have to stress two points: (i) as we demonstrated by NMR in anhydrous media, there is no tendency of the $(PO)_n$ chain to significantly change its conformation merely by heating; (ii) in aqueous media, the primary cause of the chain conformation change and subsequent self-association is the entropy-driven gradual loss of the cooperative system of hydrophobic hydration and hydrogen bonding (i.e., decrease of $(\Delta G_{hh}^{P} + \Delta G_{hb}^{P})_n$ in absolute terms) even though the further loss of these interactions can be promoted by conformation change and association of the $(PO)_n$ chain so that there is a kind of a feedback between these processes.

The same reasoning must be applicable to the $(EO)_m(PO)_n(EO)_m$ copolymers, but some additional factors have to be considered. Without a doubt, ΔH_{sol}^{E} (the superscript *E* meaning ethylene oxide or EO units) is lower in absolute terms than ΔH_{sol}^{P}, the EO unit being smaller and more polar. Also, $(\Delta G_{sol}^{E})_m$ increases less with increasing *m* due to a much higher flexibility of the $(EO)_m$ chain. There is no ΔG_{hh}^{E} term, but ΔG_{hb}^{E} is evidently somewhat higher in absolute value (probably $\Delta H_{hb}^{E} < \Delta H_{hb}^{P}$ but certainly $\Delta S_{hb}^{E} < \Delta S_{hb}^{P}$ because of the PEO chain flexibility) so that the overall ΔG^{E} remains negative in a wide range of temperatures. Thanks to this, $(EO)_m(PO)_n(EO)_m$ copolymers are soluble at normal temperature and increasing *m* shifts not only the CMT as demonstrated earlier[24] but also the preassociation conformation change of $(PO)_n$ to higher temperatures (according to the present study, the shift is 6 K when increasing *m* from 14 to 72, *n* being 31 in both cases). This "hydrophilic pull" (however attractive such a notion might be) probably does not mean any real force preventing earlier PPO conformation change but simply a larger negative cushion in the temperature dependence of ΔG. The dependence of the copolymer thermal behavior on the *m*/*n* ratio can offer another argument for the feedback connection between dehydration of PPO and its conformation change: quite in agreement with the NMR spectra, relaxation, and PFG diffusion measurements which all show the start of PPO slight coiling at 305−306 K for 14/31 and 311−312 K for 72/31, infrared spectra show[24] the first red shift of methyl deformation vibration (indicating the starting disintegration of the hydrophobic-hydration envelope) at about 303 K in the former case and at 309 for the latter one.

The negative value of ΔS_{hb}^{E} ascertains that even the PEO block will lose some of its hydrophilic character at a certain temperature. As we have shown here, parts of the block decrease their local mobility even at temperatures much lower than the CMT (the process starts at 306 K for PE6400, some 6−7 K below the CMT of this product at 10% w/w). As this relative immobilization does not apply to the PEO end-groups, we propose that mostly the "inner" (i.e., close to the junction with PPO) parts of the PEO chain become entwined with self-associating PPO, gaining thus some negative ΔG from the collective hydrophobic interactions.

Conclusions

Using ^{1}H and ^{13}C 1D and 2D NMR spectra, PFG diffusion measurements, and ^{13}C longitudinal and transverse relaxations including measurements of exchange dynamics, the temperature-dependent behavior of $(EO)_m(PO)_n(EO)_m$ block copolymers in D_2O below the critical micellar temperature (CMT) was investigated (EO and PO mean ethylene oxide and propylene oxide, respectively, and *m*/*n* was 31/14, 31/72, and 17/1).

As an aid of this study, $(PO)_8$ and $(PO)_{22}$ in D_2O and $(PO)_{35}$ in $CDCl_3$ and DMSO-d_6 were investigated. It was demonstrated that the thermal changes of the molecular shape of PPO itself are negligible in anhydrous media irrespective of its length but are strongly dependent on the chain length in aqueous solution: the 8-mer does not change in a wide range up to 322 K, whereas the 22-mer coils and associates between 293 and 295 K.

For $(EO)_m(PO)_n(EO)_m$ block copolymers in D_2O, it was shown that a conformation change of the PO block followed by mild and reversible association with other PO blocks and gradually with the inner parts of EO blocks starts at temperatures 10−12 K below CMT. In agreement with earlier infrared results, the primary process is the entropy-driven disintegration of the hydration envelope around the PPO chain originally made up by cooperation of hydrophobic hydration of the methyl groups and hydrogen bonds between water and the ether groups, as shown by model calculations. This break-up is more probable with increasing length of the PPO chain and is followed by its adopting a more staggered conformation. Both processes are mutually cooperative and microreversible with a correlation time of the order 0.01 s and the activation energy 51.3 kJ/mol. The relatively dehydrated PPO chain in a staggered conformation is prone to self-association, which starts at temperatures up to 5 K below CMT. In $(EO)_m(PO)_n(EO)_m$ block copolymers, this process is complicated by the stripping of PEO chains of a part of hydrogen-bound water and entwining the dehydrated parts with PPO chains. Only inner (PPO-near) parts of PEO take part in the process, the end-groups remaining free.

Acknowledgment. This work was supported by the Grant Agency of the Czech Republic, Project 203/09/1478.

Supporting Information Available: Program for T_2 measurements with DEPT45-excitation of ^{13}C polarization and

decoupling during acquisition. 150.94 MHz ^{13}C NMR spectra of 10% w/w PPO (P_n = 37) in dimethylsufoxide-d_6 and chloroform-*d* at the indicated temperatures. 600.2 MHz spectra of a 10% solution of $(PO)_8$ in D_2O at the indicated temperatures (in K). 150.94 MHz ^{13}C NMR spectra of 10% D_2O solution of F68 at the indicated temperatures. Purely monoexponential decays in the inversion−recovery experiment for the indicated signals of PE6400 at 306 K. Biexponential decays in the T_2 experiment for the indicated signals of PE6400 at 308 K. This material is available free of charge via the Internet at http://pubs.acs.org.

References and Notes

(1) Alexandritis, P.; Hatton, T. A. *Colloids Surf., A* **1995**, *96*, 1.
(2) Almgren, M.; Brown, W.; Hvidt, S. *Colloid Polym. Sci.* **1995**, 273.
(3) Alexandritis, P. *Curr. Opin. Colloid Interface Sci.* **1997**, *2*, 478.
(4) Chu, B.; Zhou, Z. In *Nonionic Surfactants*; Nace, V. M., Ed.; Marcel Dekker: New York, 1996; Chapter 3.
(5) *Amphiphilic Block Copolymers: Self-Assembly and Applications*; Alexandridis, P., Lindman, B., Eds.; Elsevier: Amsterdam, The Netherlands, 1997.
(6) Zhang, K.; Khan, A. *Macromolecules* **1995**, *28*, 3807.
(7) Alexandridis, P.; Olsson, U.; Lindman, B. *Macromolecules* **1995**, *28*, 7700.
(8) Alexandridis, P.; Zhou, D.; Khan, A. *Langmuir* **1996**, *12*, 2690.
(9) Wu, W.; Zhou, Z. K.; Chu, B. *Macromolecules* **1993**, *26*, 2117.
(10) Wu, W.; Chu, B. *Macromolecules* **1994**, *27*, 1766.
(11) Andersson, M.; Karlstrom, G. *J. Chem. Phys.* **1985**, *89*, 4957.
(12) Linse, P. *Macromolecules* **1993**, *26*, 4437.
(13) Hurter, P. N.; Schutjens, J. M. H. M.; Hatton, T. A. *Macromolecules* **1993**, *26*, 5030.
(14) Caragheorgheopol, A.; Schlick, S. *Macromolecules* **1998**, *31*, 7736.
(15) Patel, K.; Bahadur, P.; Guo, C.; Ma, J. H.; Liu, H. Z.; Yamashita, Y.; Kanai, A.; Nakashima, K. *Eur. Polym. J.* **2007**, *43*, 1699.
(16) Mata, J. P.; Majhi, P. R.; Kubota, O.; Khamai, A.; Nakashima, K.; Bahadur, P. *J. Colloid Interface Sci.* **2008**, *320*, 548.
(17) Wanka, C.; Hoffmann, H.; Ulbricht, W. *Macromolecules* **1994**, *27*, 4145.
(18) Zheng, L.; Guo, C.; Wang, J.; Liang, X.; Bahadur, P.; Chen, S.; Ma, J.; Liu, H. *Vib. Spectrosc.* **2005**, *39*, 157.
(19) Chan, K. L. A.; Kazarian, S. G. *Vib. Spectrosc.* **2004**, *35*, 45.
(20) Su, Y. I.; Wang, J.; Liu, H. Z. *J. Phys. Chem. B* **2002**, *106*, 11823.
(21) Su, Y. I.; Wang, J.; Liu, H. Z. *Macromolecules* **2002**, *35*, 6426.
(22) Su, Y. I.; Wang, J.; Liu, H. Z. *Langmuir* **2002**, *18*, 5370.
(23) Ma, J.; Guo, Ch.; Tang, Y.; Wang, J.; Zheng, I.; Liang, X.; Chen, S.; Liu, J. *J. Colloid Interface Sci.* **2006**, *299*, 953.
(24) Schmidt, P.; Dybal, D.; Šturcová, A. *Vib. Spectrosc.* **2009**, *50*, 218.
(25) Sasanuma, Y. *Macromolecules* **1995**, *28*, 8629.
(26) Wïhrich, K. *NMR of Proteins and Nucleic Acids*; John Wiley and Sons: New York, 1986.
(27) Cohen-Addad, J. P. *Prog. NMR Spectrosc.* **1983**, *25*, 6.
(28) Canet, D. *Nuclear Magnetic Resonance, Concepts and Methods*; John Wiley and Sons: New York, 1996.
(29) Canet, D.; Robert, J. B. *Dynamics of Solutions and Fluid Mixtures by NMR*; Delpuech, J. J., Ed.; Wiley: Chichester, U.K., 1995; p 127.
(30) Kříž, J.; Dybal, J.; Makrlík, E.; Budka, J.; Vaňura, P. *J. Phys. Chem. A* **2009**, *113*, 5896.
(31) Luz, L.; Meiboom, S. *J. Chem. Phys.* **1963**, *39*, 366.
(32) Meiboom, S.; Gill, D. *Rev. Sci. Instrum.* **1958**, *29*, 688.
(33) Wu, D.; Chen, A.; Johnson, C. S., Jr. *J. Magn. Reson., Ser. A* **1995**, *115*, 260.
(34) Frisch, M. J.; Trucks, G. W.; Schlegel, H. B.; Scuseria, G. E.; Robb, M. A.; Cheeseman, J. R.; Montgomery, J. A., Jr.; Vreven, T.; Kudin, K. N.; Burant, J. C.; Millam, J. M.; Iyengar, S. S.; Tomasi, J.; Barone, V.; Mennucci, B.; Cossi, M.; Scalmani, G.; Rega, N.; Petersson, G. A.; Nakatsuji, H.; Hada, M.; Ehara, M.; Toyota, K.; Fukuda, R.; Hasegawa, J.; Ishida, M.; Nakajima, T.; Honda, Y.; Kitao, O.; Nakai, H.; Klene, M.; Li, X.; Knox, J. E.; Hratchian, H. P.; Cross, J. B.; Bakken, V.; Adamo, C.; Jaramillo, J.; Gomperts, R.; Stratmann, R. E.; Yazyev, O.; Austin, A. J.; Cammi, R.; Pomelli, C.; Ochterski, J. W.; Ayala, P. Y.; Morokuma, K.; Voth, G. A.; Salvador, P.; Dannenberg, J. J.; Zakrzewski, V. G.; Dapprich, S.; Daniels, A. D.; Strain, M. C.; Farkas, O.; Malick, D. K.; Rabuck, A. D.; Raghavachari, K.; Foresman, J. B.; Ortiz, J. V.; Cui, Q.; Baboul, A. G.; Clifford, S.; Cioslowski, J.; Stefanov, B. B.; Liu, G.; Liashenko, A.; Piskorz, P.; Komaromi, I.; Martin, R. L.; Fox, D. J.; Keith, T.; Al-Laham, M. A.; Peng, C. Y.; Nanayakkara, A.; Challacombe, M.; Gill, P. M. W.; Johnson, B.; Chen, W.; Wong, M. W.; Gonzalez, C.; Pople, J. A. *Gaussian 03*, revision C.02; Gaussian, Inc.: Wallingford, CT, 2004.
(35) Kříž, J.; Dybal, J.; Tuzar, Z.; Kadlec, P. *J. Phys. Chem. B* **2009**, *113*, 11950.
(36) Kříž, J.; Dybal, J.; Brus, J. *J. Phys. Chem. B* **2006**, *110*, 18338.
(37) Kříž, J.; Dybal, J. *J. Phys. Chem. B* **2007**, *111*, 6118.
(38) Kříž, J.; Dybal, J.; Makrlík, E.; Budka, J. *Magn. Reson. Chem.* **2008**, *46*, 235.
(39) Kříž, J.; Dybal, J.; Makrlík, E.; Budka, J. *J. Phys. Chem. A* **2008**, *112*, 10236.

JP911205Q